HYDROLOGICAL PROCESSES
*Hydrol. Process.* (2012)
Published online in Wiley Online Library
(wileyonlinelibrary.com) DOI: 10.1002/hyp.9642

# Temporal and spatial pattern of thermokarst lake area changes at Yukon Flats, Alaska

Min Chen,[1]* Joel C. Rowland,[1] Cathy J. Wilson,[1] Garrett L. Altmann[1,2] and Steven P. Brumby[3]

[1] *Division of Earth and Environmental Sciences, Los Alamos National Laboratory, Los Alamos, NM, USA*
[2] *Department of Forest Sciences, University of Alaska, Fairbanks, AK, USA*
[3] *Division of Intelligence and Space Research, Los Alamos National Laboratory, Los Alamos, NM, USA*

## Abstract:

To better understand the linkage between lake area change, permafrost conditions and intra-annual and inter-annual variability in climate, we explored the temporal and spatial patterns of lake area changes for a 422 382-ha study area within Yukon Flats, Alaska using Landsat images of 17 dates between 1984 and 2009. Only closed basin lakes were used in this study. Among the 3529 lakes greater than 1 ha, closed basin lakes accounted for 65% by number and 50% by area. A multiple linear regression model was built to quantify the temporal change in total lake area with consideration of its intra-annual and inter-annual variability. The results showed that 80.7% of lake area variability was attributed to intra-annual and inter-annual variability in local water balance and mean temperature since snowmelt (interpreted as a proxy for seasonal thaw depth). Another 14.3% was associated with long-term change. Among 2280 lakes, 350 lakes shrank, and 103 lakes expanded. The lakes with similar change trends formed distinct clusters, so did the lakes with similar short term intra-annual and inter-annual variability. By analysing potential factors driving lake area changes including evaporation, precipitation, indicators for regional permafrost change, and flooding, we found that ice-jam flooding events were the most likely explanation for the observed temporal pattern. In addition to changes in the frequency of ice jam flooding events, the observed changes of individual lakes may be influenced by local variability in permafrost distributions and/or degradation. Copyright © 2012 John Wiley & Sons, Ltd.

KEY WORDS thermokarst lakes; temporal and spatial analysis; climatic change; ice-jam flooding; permafrost; Yukon Flats in Alaska

*Received 24 January 2012; Accepted 29 October 2012*

## INTRODUCTION

Thermokarst lakes are common in Alaska (Smith *et al.*, 2007; Arp and Jones, 2009), and they are particularly abundant on the Arctic Coastal Plain (Frohn *et al.*, 2005; Hinkel *et al.*, 2005; Jones *et al.*, 2009) and central and western Alaska (Jorgenson and Osterkamp, 2005; Riordan *et al.*, 2006; Jones *et al.*, 2011). They are an important component in arctic landscape because of their critical role in regional hydrologic and biogeochemical cycles (especially methane emission), energy balances, human water and food supply and wildlife habitat provision (Boyd, 1959; Kling *et al.*, 1992; Rovansek *et al.*, 1996; Bowling *et al.*, 2003; Cott *et al.*, 2008; Jones *et al.*, 2009; Bowling and Lettenmaier, 2010). The development, expansion and drainage of thermokarst lakes depend on the lateral and vertical degradation of permafrost (Hinzman *et al.*, 2005). Consequently, areal changes in thermokarst lakes can reflect changes in the spatial distribution and depth of permafrost. Several studies have been conducted to detect long-term trend in lake area change in Alaska. For example, 22 of 24 ponds shrank between 1950 and 2000 in a study area near Council (Yoshikawa and Hinzman, 2003); a reduction (4%–31%) in the area of shallow, closed-basin ponds was observed in eight boreal regions throughout Alaska and an area increase of 1% was reported in Arctic Coastal Plain between 1950s and 2002 (Riordan *et al.*, 2006); total lake area decreased by 14.9% for a 70 000-ha study area in northern Seward Peninsula between 1950/1951 and 2006/2007 (Jones *et al.*, 2011); 6 of 9 lakes decreased in area (by 2.2%–57.9%) between 1952 and 2000 at Yukon Flats (Corcoran *et al.*, 2009); the total area of closed water bodies (greater than 3600 $m^2$) has decreased by 0.07% throughout the Yukon River Basin from 1984–1989 to 2003–2008, although different trends were observed in continuous and discontinuous permafrost regions (Lu and Zhuang, 2011); 3.4% of more than 15 000 water bodies showed a net decrease in the area extent in central Alaska from 1979 to 2009 (Rover *et al.*, 2012). However, no significant trend in lake area change was observed in the National Petroleum Reserve Alaska (Jones *et al.*, 2009). Permafrost degradation was regarded as the main driving factor of lake area decrease in some studies (Yoshikawa and Hinzman, 2003; Jones *et al.*, 2011), whereas in other studies, increasing evapotranspiration and extended growing season were also thought to be important drivers (Riordan *et al.*, 2006; Corcoran *et al.*, 2009). It is obvious that permafrost degradation is not the only factor that influences thermokarst lakes; other factors observed to have impacts on lake areas include the following: precipitation and evaporation

*Correspondence to: Min Chen, Division of Earth and Environmental Sciences, Los Alamos National Laboratory, Los Alamos, NM, USA
E-mail: min@lanl.gov

(Bowling *et al.*, 2003; Plug *et al.*, 2008; Corcoran *et al.*, 2009; Jones *et al.*, 2009; Labrecque *et al.*, 2009; Bowling and Lettenmaier, 2010), hydrologic connectivity to rivers (Riordan *et al.*, 2006; Anderson *et al.*, 2007; Roach *et al.*, 2011), and flooding (Marsh and Lesack, 1996; Lesack and Marsh, 2007). Because of limited availability of remote sensing images and intense work involved in extracting lakes from those images, most investigations on lake area change have directly compared lake areas over two to four periods, without consideration of intra-annual and inter-annual variability in lake areas that might be caused by other factors. Rover *et al.* (2012) used multi-date measurements of the extents of individual lakes to analyse lake area change trend, but the seasonality was still not taken into account. Lack of consideration of intra-annual and inter-annual variability can thus limit our ability to infer causal mechanisms of lake area change and prevent us from separating long-term trends from inter-annual variability (Plug *et al.*, 2008; Corcoran *et al.*, 2009; Jones *et al.*, 2009; Arp *et al.*, 2011). Therefore, studies with higher temporal resolution and a full consideration of multiple factors impacting lake areas are needed to detect and quantify the long-term trend in lake area changes possibly caused by permafrost degradation as well as other climate-driven factors (Labrecque *et al.*, 2009; Arp *et al.*, 2011).

Besides the long-term trend in lake area change at regional scale, spatial heterogeneity in lake behaviors has also been of increasing interest. Riordan *et al.* (2006) pointed out that even within a single aerial photograph in Yukon Flats, some ponds remained stable while neighboring ponds showed a substantial area decrease between 1950s and 2000 with the observed lake drainage related to warming permafrost. Jones *et al.* (2009) studied lakes in the National Petroleum Reserve Alaska and found that areal change of individual lakes was also highly influenced by lake bathymetry and hydrogeomorphology. Jones *et al.* (2011) analysed lake dynamics for a 70 000-ha area in northern Seward Peninsula and concluded that lake drainage was triggered by lateral breaching but not subterranean infiltration. Roach *et al.* (2011) compared eight lake characteristics for 15 lake pairs to identify the primary mechanisms underlying heterogeneous trends in closed-basin lakes and concluded that terrestrialization/evapotranspiration was the primary mechanism for lake area reduction, and thermokarst was the primary mechanism for non-decreasing lakes (lakes that either expanded or did not change). This inter-lake variation can mask or skew detection of total lake area change at regional scale (Arp *et al.*, 2011). Investigation of inter-lake variation in area change may also help provide a better understanding of the hydrologic and geomorphic processes within a region (Arp *et al.*, 2011).

To better understand the linkage between lake area, permafrost and intra-annual and inter-annual variability in climate, we selected a 422 382-ha study area southwest of the Yukon River to explore the temporal and spatial patterns in lake area changes from 1984 to 2009. The goal of our study was to detect whether there was statistically significant long-term trend in lake area change and whether the lakes with similar change trends were clustered at certain locations or randomly distributed. If there were significant temporal trend and spatial patterns, we sought to identify key drivers for the temporal and spatial patterns. By exploring this relatively long-term dataset that accounts for intra-annual, inter-annual and decadal changes, we hope to improve the prediction of lake area changes at different spatial locations and local climatic conditions.

## STUDY AREA

Our study area (longitude: 145.10°-149.23°W; latitude: 65.91°- 66.59°N; total area: 422 382 ha; Figure 1) is located in the Yukon Flats of Yukon Flats National Wildlife Refuge and south and west to the Yukon River. The area has low relief with elevations ranging from 88 m above mean sea level in the west and north to 150 m in the east and south. The climate in the study area is classified as cold continental,

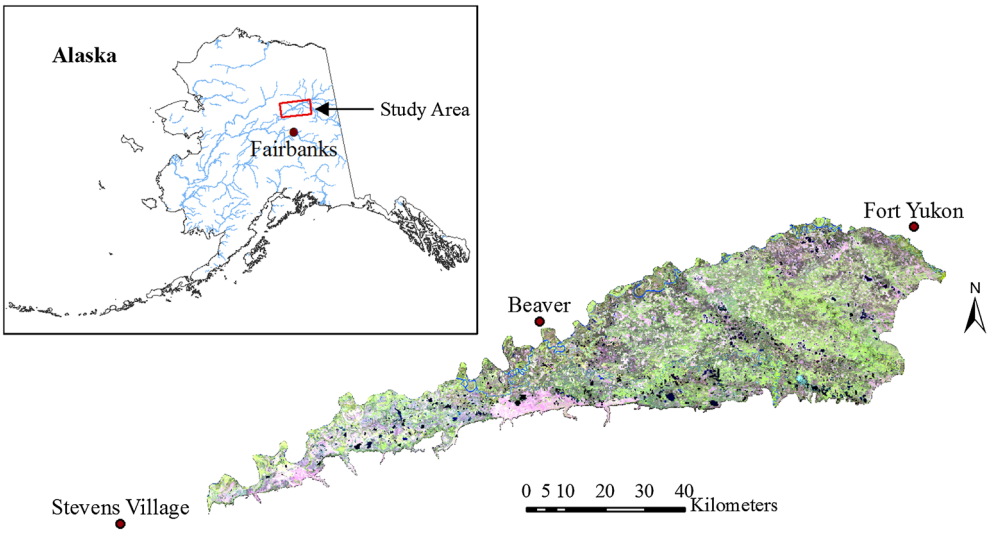


Figure 1. Location and Landsat imagery (August 16, 2000) of the study area

characterized by extremes of temperature between summer and winter, long cold winters, warm summers, low precipitation and high evaporation (Williams, 1962; Ford and Bedford, 1987). Calculated from 1951–2009 weather record (National Climatic Data Center, NOAA Satellite and Information Service) at Fairbanks International Airport located about 150 km to the south of study area, the mean annual air temperature is −3°C, with mean January temperature of −23°C and mean July temperature of 17°C. Annual precipitation is 26.72 cm water equivalent, based on 1951–2000 weather record at Fairbanks International Airport, with 35% as snowfall. Snow covers the ground from October through April. Because of relative high summer evaporation rate, this region often has a negative annual water balance (Ford and Bedford, 1987). This area lies below the regional timberline, with spruce and birch forest along the Yukon River and its tributaries and a mixture of forest with muskeg and marsh distributed away from the rivers (Williams, 1962).

The study area is underlain by discontinuous permafrost (Jorgenson *et al*., 2008), which is relatively warm and thin, and thus particularly sensitive to the effects of climate change (Osterkamp and Romanovsky, 1999; Jorgenson *et al*., 2001; Lewkowicz *et al*., 2011). The permafrost layer acts as an aquiclude, which substantially affects surface and subsurface hydrology. In particular, it impedes surface water drainage into the subsurface and helps to maintain an abundance of relatively shallow lakes and wetlands that would be less common for the dry climate in interior Alaska (Roach *et al*., 2011). At one location near the northeast boundary of the study area, permafrost is about 60–119 meters deep, whereas in the northwestern area along Yukon River, permafrost is present, but depth is unknown (Williams, 1962; Jorgenson *et al*., 2008). Ground ice is common in alluvial-fan silt, loess, locally distributed in the silt deposits of the alluvial fans and related terraces, as well as in flood-plain and low-terrace silt (Williams, 1962). Overall, however, the distribution and thickness of permafrost in the study area is poorly constrained.

Lakes in Yukon Flats are mainly of two origins: thermokarst lakes and oxbows (Arp and Jones, 2009). Thermokarst lakes formed in depressions created by permafrost degradation, whereas oxbows formed by meander cut-offs. The oxbows may or may not be underlain by permafrost, so the potential influence of permafrost on individual lake dynamics is uncertain. Although thermokarst lakes formed as a result of permafrost degradation, it is not necessary that thermokarst lakes are underlain by permafrost. In regions of warm, thin permafrost, the presence of the lakes may lead to ground temperature increase and complete thawing of permafrost beneath the lakes (Yoshikawa and Hinzman, 2003; Jorgenson *et al*., 2010; Rowland *et al*., 2011).

## DATA AND METHODS

We examined the change in area for a subset of closed-basin lakes (without detectable connection to rivers) during a 25-year period from 1984 to 2009. Landsat images from a total of 17 dates were used to obtain areal extent of all the lakes, and then high-resolution satellite imagery (~2 m/pixel) from 2006 to 2010 was used to identify closed basin lakes greater than 1 ha. With a time series of total areas of closed basin lakes, we were able to detect long-term lake area change trends for the study region, using a multiple linear regression model, with consideration of intra-annual and inter-annual lake area variability. Spatial patterns of individual lake area changes were also identified. Finally, possible controls on both the long-term changes and the patterns of spatial variability were examined. These controls included the following: ice-jam flooding, regional permafrost degradation, local permafrost distribution, precipitation and air temperature.

Year 1984 was chosen as the starting point to track lake area change because the first cloud-free Landsat TM/ETM + image for this study region was available in 1984 and the year 1984 also coincided with the start of the most recent warming period (mid-1980s to present) across Alaska (Osterkamp, 2007). Only closed-basin lakes were used because we hypothesized that their sensitivity to changes in precipitation, evaporation and permafrost degradation related to climatic change and their areal changes are less likely impacted by highly variable stage level of streams or rivers (Riordan *et al*., 2006; Roach *et al*., 2011).

### *Landsat images*

Landsat TM/ETM + images with a spatial resolution of 30 × 30 m, obtained from United States Geological Survey website (http://glovis.usgs.gov/), were used to obtain lake areal extent from 17 dates from 1984 to 2009 (Table I). These 17 dates were grouped into 4 periods: I) 1984–1986, II) 1994, III) 1999–2002 and IV) 2009. For each date, two to four scenes were used to cover the whole study region. In images with gaps because of clouds and cloud shadows, we used unobstructed portions of images from the next closest available date to fill these gaps to obtain complete lake coverage (Table I).

We used Genie Pro (Brumby *et al*., 1999; Perkins *et al*., 2005), an automated feature detection/classification system, to extract lakes from those Landsat images (bands 1–5 and 7 were used). Genie Pro uses an evolutionary algorithm to generate textural-spectral image processing pipelines to classify multi-spectral imagery. In particular, Genie Pro integrates spectral information and spatial cues, such as texture, local morphology and large-scale shape information, and allows human experts to interact efficiently with the software through an interactive and iterative 'training dialog'(Perkins *et al*., 2005). Detailed description of classification algorithms of Genie Pro can be found in Perkins *et al.* (2005). Compared with traditional supervised classifiers, Genie Pro shows consistently better performance with regard to the correct identification of target pixels and nontarget pixels by exploiting both color/spectral and spatial textural signatures in moderate-resolution multi-spectral imagery (Harvey *et al*., 2002). Genie Pro was trained using human mark-up of about 20 lakes out of thousands of lakes

Table I. Imagery dates

| Periods | Dates |
|---|---|
| **I: 1984-1986** | August 12, 1984 |
| | July 30, 1985 |
| | June 15, 1986 |
| **II: 1994** | September 9, 1994 |
| **III: 1999-2002** | June 26 and 28, 1999 |
| | August 16 and 22, 1999 |
| | September 6 and 8, 1999 |
| | June 4 and 6, 2000 |
| | June 13, 2000 |
| | July 6 and 8 2000 |
| | August 16, 2000 |
| | June 16, 2001 |
| | September 20, 2001 |
| | July 21, 2002 |
| | August 6, 2002 |
| **IV: 2009** | July 16, 2009 |
| | August 17, 2009 |

(or ~0.5% of all pixels) in the study area as an initial step, and a map of lake pixels was produced by the Genie Pro algorithm. We manually inspected the map to determine classification accuracy and revised the training class until Genie Pro generated a solution that best classified the lakes. Because of a lack of ground-verified inventory of lake areas for our image dates (or any date), it is not possible to determine a quantitative assessment of classification errors. An example lake extraction result was shown in Figure 2. By using consistent criteria for training the automated classification lake pixels on all image dates, the errors because of subjective classifications were minimized. A small subset of lakes (~40) was covered by emergent vegetation in the summer, which made both automated and manual detection of water surface very difficult. Those lakes were easy to identify from Landsat images as their surface changed dramatically from June to August each year. Specifically, their water surface were usually very large and distinctly appeared as one lake (blue/dark patches on the images) in June, but in August, the lakes became patchy though the original shore line remained the same as in June, with a large portion of the lake surface replaced by vegetation (green patches within individual lake boundary on the images). Therefore, those lakes were excluded in this study.

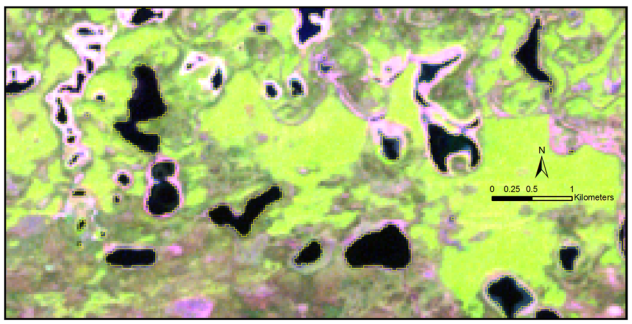


Figure 2. Lake extraction result generated by Genie Pro. Here, polygons generated from the outer boundary of blocks of lake pixels identified by Genie Pro are shown. Only part of the extraction result was included in the figure to clearly show the lakes on Landsat image and lakes extracted by Genie Pro

To track area change of individual lakes, we assigned an identification (ID) number to each lake and calculated its area for each date. By merging lakes from all dates into one raster using Arcgis 9.3.1, we were able to create the maximum potential lake size for each lake. Then, using Fragstats (Spatial Pattern Analysis Program for Categorical Maps, developed by University of Massachusetts (McGarigal *et al.*, 2002)), an ID number was generated for each region of spatially contiguous lake pixels in the raster with maximum potential lake size. The lakes from the maximum potential lake raster were then converted into discrete polygons and assigned the ID numbers generated from Fragstats. Lakes from raster dataset were converted to polygons, and lake areas were calculated in Arcgis for each of the 17 dates. These polygons were then spatially joined to the target polygon with potentially maximum lake size. Because the IDs were generated from the raster with the maximum potential lake size, some lakes may appear as one whole lake in the early summer but fall into multiple parts in late summer. The areas of the multiple parts were summed together to represent the areal extent of a particular lake. In this way, we tracked areal change of individual lakes as well as total lake area change for the whole region.

Lakes with maximum area greater than 1 ha were examined for their origin (oxbow or thermokarst) and connectivity to rivers. We visually examined the shape of lakes. If the lakes had a U-shape and appeared associated with the surrounding river or stream channels, then they were considered oxbow lakes and excluded from further analysis. Because channels connecting lakes to rivers were too small to detect using Landsat imagery, we used high resolution satellite imagery (~2 m/pixel) from 2006 to 2010 to identify non-closed basin lakes among the thermokarst lakes. Only closed basin lakes not considered oxbows were used for further temporal and spatial analysis of lake area change.

### *Meteorological data*

Two NOAA weather stations, located near Beaver and Fort Yukon in Alaska (http://www.ncdc.noaa.gov/oa/ncdc.html), are the closest stations to our study area. However, neither of the two stations has complete weather record for our study period from 1984 to 2009. Specifically, Beaver station had data from 1997 to 2000 and Fort Yukon had data from 1984 to 1990, and both stations had significant missing data. Two Remote Automated Weather Stations (RAWs, http://www.wrcc.dri.edu/wraws/akF.html), located at Beaver and New Lake, are within our study area and they have relatively complete daily air temperature, humidity and wind speed records; however, the RAWs data were not available for the years before 1990. The precipitation data were only available for summer months at these two RAWs. The relatively complete daily precipitation data were available at Fort Yukon station (SNOTEL site, http://www.wcc.nrcs.usda.gov/snow/snotel-precip-data.html), but it did not cover the years before 1990. In addition, the precipitation data from different sources had great discrepancy, for example, the mean annual precipitation at Fort Yukon was 162 mm from NOAA database but 207 mm

from SNOTEL database. Because it seemed unreasonable to simply combine data from different sources to obtain a comparable time series of precipitation data, we chose the next closest NOAA weather station, Fairbanks International Airport, with complete weather dataset through our study period available at National Climatic Data Center (http://www.ncdc.noaa.gov/oa/ncdc.html). Although Fairbanks International Airport is about 150 km south of the study area, its elevation (131 meters) and climate are very similar to those of our study area. High correlation ($r = 0.97$) of daily mean temperature between Beaver (from both NOAA database and RAWs database) and Fairbanks International Airport was observed. Similar annual precipitation at Beaver station (NOAA database) and Fairbanks International Airport were observed in 1997 and 1998 (years for which there was the smallest number of missing values at Beaver station). In addition, for monthly precipitation, the correlation coefficients were 0.6 between SNOTEL Fort Yukon station and Fairbanks station. Therefore, we consider the weather record at Fairbanks International Airport as representative for our study area.

To assess the impact of local water balance on lake areas, we evaluated the local precipitation (P) and evaporation (E) to calculate local water balance. Daily precipitation can be directly obtained from Fairbanks weather record. Daily evaporation was calculated from maximum, minimum and mean air temperature (°C), average dew point temperature (°C), wind speed (m $s^{-1}$), cloud cover (range, 0–1) at Fairbanks station using a simple finite difference model (Finch and Gash, 2002). This simple finite difference model took the heat stored in the water body and sensible heat flux into consideration and was able to accurately estimate water temperature and evaporation for open water surface, as seen from excellent agreement between the predicted and measured values of both evaporation and water temperature (Finch and Gash, 2002). The importance of heat stored in the water body and sensible heat flux to the calculation of evaporation at high latitude regions has been highlighted in prior studies (Shuttleworth, 2012).

The water temperature and evaporation were calculated by iteration in the simple finite difference model. For each iteration step, the latent heat flux, sensible heat flux and heat stored in the water body were calculated based on estimated water temperature. Detailed calculation of water temperature ($T_w$) and evaporation ($E$) can be found in section 2.2 of the paper by Finch and Gash (2002). Detailed calculation of net radiation ($R_n$) as a required input by the finite difference model can be found in Chapter 5 of Shuttleworth (2012). Here, we only listed the important equations used in each iteration step. For each day (time step), $R_n$ was first calculated using Equation 1. Equations 2 to 8 were iterated until the difference between estimates of the water temperature at the end of the current time step ($T_{w,i}$) on successive iterations is less than 0.01 °C (Finch and Gash, 2002). Daily $E$ was calculated only for the period from May to September, and it was assumed to be zero for other months because of widespread snow cover and low temperature throughout the winter.

$$R_n = S_n^d + L_n^d \tag{1}$$

$R_n, S_n^d, L_n^d$ refer to net radiation, net short-wave radiation and net long-wave radiation, respectively (all in MJ $m^{-2}$ $d^{-1}$). $R_n, S_n^d, L_n^d$ were calculated using mean air temperature (°C), maximum air temperature (°C) and minimum air temperature (°C), cloud cover (0 to 1), Julian date (1 to 365/366), latitude (1.131264 radians = 64.8 ) and albedo (0 to 1), as explained in details in Chapter 5 of Shuttleworth (2012). The water surface albedo is a function of the Sun's altitude (degree) and the atmospheric transmittance (Payne, 1972). We obtained the daily average Sun's altitude (averaged for the hours from 6:00 to 18:00 for each day) at Fairbanks from U.S. Naval Observatory Website (http://aa.usno.navy.mil/data/docs/AltAz.php). The atmospheric transmittance was assumed to be 0.5 for our study area, corresponding to partially cloudy condition (Payne, 1972). From a table of measured values, the appropriate daily albedo value was obtained (Payne, 1972). The albedo used in our calculation ranged from 0.071 (late June) to 0.295 (late September).

$$T_w = T_{w,i-1} + \left(T_{w,i} - T_{w,i-1}\right)/2 \tag{2}$$

$T_w$ is the average water temperature (°C), $T_{w,i}$ and $T_{w,i-1}$ are the estimated water temperature (°C) at the current time step and the previous time step, respectively. For the first iteration of each day, $T_w$ was set to be equal to the value obtained from the last iteration of previous time step. After one iteration from Equations 2–8, $T_{w,i}$ is updated for the current day, and the iteration will continue until difference in $T_{w,i}$ between successive iterations is less than 0.01°C.

$$f(u) = \frac{0.216u}{\Delta + \gamma} \qquad if\ T_w \le T_a \tag{3}$$

$$f(u) = \frac{0.216u\left[1 + \frac{10(T_w - T_a)}{u^2}\right]^{0.5}}{\Delta + \gamma} \qquad if\ T_w > T_a \tag{4}$$

$f(u)$ (MJ $m^{-2}$ $d^{-1}$ $kPa^{-1}$) is the wind function, depending on whether $T_w$ is less than or equal to $T_a$, it may take of the form of Equation 3 or 4. $T_a$ refers to the mean air temperature (°C). $\Delta$ (kPa °C $^{-1}$) is the slope of the saturation water vapor- temperature relationship at air temperature, and $\gamma$ (kPa °C $^{-1}$) is psychrometric constant. $f(u)$ is calculated based on $u$, wind speed at 10 m (m $s^{-1}$). The wind speed at Fairbanks was measured at 33 feet (10 m) in 1984 and the years after 1997 but at 30 feet (9 m) in 1985, 1986 and 1994, so we calculated the wind speed at 10 m for 1985, 1986 and 1994 using the equations from Chapter 23 of Shuttleworth (2012). The detailed calculation of $\Delta$ and $\gamma$ can be found in Chapter 2 and Chapter 23 of Shuttleworth (2012).

$$\lambda E = f(u)\left(e_w^* - e_d\right) \tag{5}$$

$$H = \lambda f(u)(T_w - T_a) \tag{6}$$

$$W = R_n - \lambda E - H \tag{7}$$

$$T_{w,i} = T_{w,i-1} + \frac{W}{\rho c h} \tag{8}$$

$\lambda E$, H and W are the latent heat flux, sensible heat flux and the heat stored in the water body (all in MJ $m^{-2}$ $d^{-1}$). $e_w^*$ and $e_d$ refer to the saturated and actual average vapor pressure, respectively (kPa). $\rho$ is the density of water (1000 kg $m^{-3}$), $c$ is the specific heat of water (0.0042 MJ $kg^{-1}$ $K^{-1}$) and $h$ is the depth of the water, which was assumed to be 2 m in this study. Detailed calculation of $e_w^*$ and $e_d$ can be found in Chapter 23 of Shuttleworth (2012). $\lambda$ is the latent heat of vaporization of water (MJ $kg^{-1}$), which can be calculated using water temperature $T_{w.i}$, as described in Chapter 2 of Shuttleworth (2012). $E$ is the daily evaporation rate (mm $d^{-1}$). We calculated $E$ by rewriting Equation 5, as follows:

$$E = \frac{f(u)\left(e_w^* - e_d\right)}{\lambda} \tag{9}$$

Monthly mean temperature and precipitation data for 1984–2009 was also obtained from the National Climatic Data Center (http://www.ncdc.noaa.gov/oa/ncdc.html) to analyse the climatic change trend between different periods.

Ice-jam flooding information was obtained from National Weather Service, Alaska-Pacific River Forecast Center (http://aprfc.arh.noaa.gov). Flood records at Fort Yukon and Beaver Village were used in this analysis because they are adjacent to our study region. We calculated the ice-jam flooding frequencies at Fort Yukon and Beaver Village for each period, by dividing the total number of ice-jam events reported in each period by the duration of the period in years. Ice-jam flooding in years 1979–1986, 1987–1994, and 1995–2002 was included in Periods I, II and III, respectively. Ice-jam flooding in years 2003–2009 was included in Period IV.

Borehole data at Yukon Bridge (Lat: 65.8804° N, Long: 149.7099°W) for the period of 1993–2002 and 2005–2009 was downloaded from NCAR/EOL website (URL: http://data.eol.ucar.edu/codiac/dss/id=106.ARCSS907) and The Geophysical Institute Permafrost Laboratory (GIPL) website (URL: http://permafrost.gi.alaska.edu/site/yb1), respectively. Among the 27 permafrost observatories in Alaska (Osterkamp, 2007), Yukon Bridge is the closest to our study region (about 30 km to the southwestern boundary), and thus, its permafrost temperature was the most representative for our study region.

Active layer depth data at 3 sites (Wickersham, Bonanza Creek LTER and Pearl Creek) near Fairbanks for the period of 1990–2009 were obtained from the Circumpolar Active Layer Monitoring (CALM) website (http://www.udel.edu/Geography/calm/data/north.html).

*Temporal analysis*

Temporal analysis was conducted for the total areas of closed basin thermokarst lakes over a 25-year period. The goal of temporal analysis was to detect if there was statistically significant long-term lake area change in the region and, if so, determine the factors responsible for this change. In addition to permafrost degradation, other studies have observed large intra-annual and inter-annual variability in lake areas caused by changes in the local water balance (Bowling *et al.*, 2003; Arp *et al.*, 2011; Chen *et al.*, In Review). Therefore, to quantify how each factor affects total lake area, we simultaneously accounted for intra-annual, inter-annual variability as well as long term lake area change trend by using a multiple linear regression models:

$$\mathrm{TLA} = a + b_1 \bullet \mathrm{LWB} + b_2 \bullet \mathrm{MTSS} + b_{3i} \bullet \mathrm{PRD} + e \tag{10}$$

where TLA is total lake area (ha); LWB is local water balance (cm), measured by cumulative P-E since preceding October; MTSS is mean air temperature since snowmelt (°C), calculated by taking the average of daily mean temperature over the period from 1 May to the date when Landsat image was acquired. PRD is a dummy variable and represents different periods, including 1984–1986, 1992, 1999–2002, 2009. 'a' is the intercept, and '$b_1$, $b_2$, $b_{3i}$' are the coefficients of those predictors, where $i$ indicates different periods. $e$ is the error term.

Local water balance was used to account for intra-annual and inter-annual variability in lake areas. Cumulative P-E since preceding October was employed to represent local water balance because past hydrologic process studies showed that the Arctic water balance is tightly coupled to snowmelt recharge in the late spring and then to evaporation in excess of precipitation in the summer (Bowling *et al.*, 2003; Woo and Guan, 2006; Arp *et al.*, 2011). Summer mean air temperature has been documented to have a strong influence on the active layer depth because strong correlation has been observed between them in previous studies (Zhang *et al.*, 1997; Guglielmin, 2004; Conovitz *et al.*, 2006; Bockheim *et al.*, 2007; Davydov *et al.*, 2008; Adlam *et al.*, 2010). Therefore, we believed that the seasonal thaw depth could also be greatly controlled by mean air temperature since snowmelt, although it could also be affected by other factors such as snowpack depth (Mackay, 1995), soil moisture (Hinkel *et al.*, 2001) and summer wind speed (Adlam *et al.*, 2010). For this study, mean air temperature since snowmelt was calculated as the average temperature from 1 May to the date of the Landsat image and used in our model as a partial proxy for the seasonal thaw depth within the active layer. Thaw depth may affect lake area in two ways (Woo and Guan, 2006). First, as the frost table deepens, a greater proportion of rainfall or snowmelt water may infiltrate into the soil rather than enter lakes as surface runoff. As a result, given the same amount of rainfall or snowmelt, a deeper frost table leads to smaller lake areas. Second, deepening of the thaw zone beneath and around lakes can enhance vertical seepage and lateral drainage, both of which will decrease lake areas. Because there is intra-annual and inter-annual variability in seasonal thaw depth, mean air temperature since snowmelt also indirectly accounted for intra-annual and inter-annual variability in lake areas. With the intra-annual and inter-annual variability

accounted for by local water balance and mean air temperature since snowmelt, we were able to detect whether there were significant long-term areal change between the four time periods. Thus, $b_{3i}$ measures the importance of long-term effects of other factors on lake area, independent from intra-annual or inter-annual variability in local water balance and mean air temperature since snowmelt (partial proxy for seasonal thaw depth).

Daily mean air temperature was used for the calculation of both evaporation and mean air temperature since snowmelt, which might cause multicollinearity in the model. However, in the model, the water balance (P-E) was used instead of E itself, and the correlation coefficient between water balance and mean air temperature since snowmelt was −0.75, and the R squared was 0.55, which meant 55% of variability of one variable could be explained by the other and 45% of variability was not explained. In the linear regression model, the variance inflation factor (VIF, which is usually used to test the multicollinearity of independent variables) was 4.2 for water balance and 2.7 for mean air temperature since snowmelt, well below the commonly used threshold of 5 or 10 (Menard, 1995; Neter *et al.*, 1996). Therefore, the potential for multicollinearity to invalidate our model appeared limited.

Statistical software R 2.13.1 was used to conduct the regression analysis, analysis of variance and trend analysis. Assumptions of linear regression were regarded as satisfied because the residuals were independently and normally distributed, with constant variance for all the predictions.

### *Spatial analysis*

We quantitatively examined the spatial patterns of lake area changes to look for regions of greater variation and change that may be indicative of local controls on lake hydrology such as ice-jam flooding, geology and permafrost distribution. The years 1994 and 2009 were not included in the spatial analysis because there were only one or two dates when the clouds-free Landsat images were available in those years, making areal extent of individual lakes less representative.

In addition to local water balance and seasonal thaw depth, the areal extent of individual lakes may also be affected by local geological and topographical characteristics (Yoshikawa and Hinzman, 2003; Roach *et al.*, 2011). Consequently, the intra-annual and inter-annual variability of individual lakes cannot be accounted for by using only local water balance and mean air temperature since snowmelt (partial proxy for seasonal thaw depth). However, detection of a long term trend cannot be done without consideration of natural fluctuation of lake areas. Therefore, we first determined the intra-annual and inter-annual range of areal extent of individual lakes within each period and then detected their change trends by comparing their intra-annual and inter-annual range between the two periods. In this study, we detected shrinking lakes and expanding lakes in a conservative way as follows. A lake was classified as a shrinking lake if its smallest area extent during 1984–1986 was bigger than the largest area extent during 1999–2002, and the shrinking area was calculated from the difference between the minimum area at Period I and the maximum area at Period III. A lake was classified as an expanding lake if its largest area extent during 1984–1986 was smaller than the smallest area extent during 1999–2000 and the expanding area was calculated from the difference between the maximum area at Period I and the minimum area at Period III. Lakes that did not fall into either of these two categories were classified as 'no change' and were assigned a change area of zero. In ArcGIS, Global and local Moran's I (Anselin, 1995) were used to measure the spatial autocorrelation of lake area change and identify clusters of lakes with the same change trends.

In addition to detection of long term lake area change from Period I to Period III, we also investigated the short term intra-annual and inter-annual variability of individual lakes using data from Period III only. From the short term variability in lake areas, we may be able to infer how lakes are influenced by geological factors such as permafrost distribution. Specifically, we tracked the lake areas and calculated their coefficients of variation (CV) by dividing the standard deviation of lake areas by the mean of lake areas for each individual lake in Period III (11 dates between 1999 and 2002). Local Moran's I (Anselin, 1995) was also used to identify clusters of variable lakes (characterized by high CV) and stable lakes (characterized by low CV).

After mapping the shrinking, expanding and unchanged lakes, we tested whether the variations in the trends of change depended on their surface geology mapped by Karlstrom *et al*. in 1964 (U. S. Geological Survey and Karlstrom, 1964) using Pearson's chi square test, a statistical test used for testing whether two variables are associated or independent.

## RESULTS

A total of 8580 lakes, with a potential maximum area extent (sum of maximum area for each lake) of 40 185 ha, were detected over our study period (excluding lakes with large emergent vegetation) (Table II). In terms of quantity, there were 5051 small lakes (< 1 ha), which accounted for 58.9% of total number of lakes, however, they only accounted for 3.9% of total lake area. For the 3,529 big lakes (≥ 1 ha), we classified them into two types, oxbow and thermokarst lakes. By visually examining lake shape, we identified 732 oxbow lakes and 2797 thermokarst lakes. From the thermokarst lakes, 493 lakes were classified as non-closed basin, and 2280 lakes were classified as closed basin lakes by checking connectivity between lakes and rivers using high-resolution remote sensing images. Only the 2280 closed basin lakes, which accounted for 47.9% of total lake area, were included for further temporal and spatial analysis.

### *Temporal trend of total lake area change*

We documented substantial intra-annual and inter-annual as well as inter-period variations in total area of closed basin thermokarst lakes over this 25-year study period (Figure 3, observed lake areas), with a mean area of 11 120 ha,

Table II. Lake inventory

| Lake size | Lake type | | Quantity (%) | Area (ha) (%) |
|---|---|---|---|---|
| All | | | 8580 (100) | 40 185 (100) |
| Small lakes (<1 ha) | | | 5051 (58.9) | 1575 (3.9) |
| Big lakes (≥1 ha) | | | 3529 (41.1) | 38 610 (96.1) |
| | Oxbow lakes | | 732 (8.5) | 5878 (14.6) |
| | Thermokarst lakes | | 2797 (32.6) | 32 732 (81.5) |
| | | Not examined | 24 (0.3) | 34 (0.1) |
| | | No closure | 493 (5.7) | 13 434 (33.4) |
| | | **Closed basin** | **2280 (26.6)** | **19 264 (47.9)** |

*Note*: Lake areas were calculated from the polygon of potentially maximum lake area extent.

standard deviation of 2109 ha and coefficient of variation of 0.19. Lake areas were generally the largest in June and then gradually declined in July and August. In September, lake area increased slightly compared with August, although we only had one year (1999) in which Landsat images were available for both August and September. At the same time, the local water balance (measured by cumulative P-E since preceding October), and mean air temperature since snowmelt also varied greatly over the study period (Figure 4). Commonly, water balance was highest in June and then decreased dramatically throughout the summer, caused by evaporation in excess of precipitation. However, the water balance of early summer season (June) was not always higher than that of later summer season (July to September) between different years. For example, the water balance on 30 July 30 1985 was higher than 15 June 1986, and the water balance on 21 July 2002 was higher than that on 28 June 1999. The average annual evaporation at Fairbanks calculated based on the simple finite difference model was 335 mm, with standard deviation of 36 mm. The average annual Pan evaporation at Rampart no. 2 station during 1963–1978 (Western Regional Climate Center, URL: http://www.wrcc.dri.edu/htmlfiles/westevap.final.html), 138 km northwest to Fairbanks, was 424 mm. The ratio of average annual lake evaporation we calculated to the average annual pan evaporation recorded for Rampart no. 2 station was 0.79, close to the average ratio of 0.7 used for the western United States (Brutsaert and Yeh, 1970).

Regression analysis of total lake area against local water balance, mean air temperature since snowmelt and period showed that these three variables explained 95.0% of total variance in lake areas, and they were all significant at a level of 0.05 (Table III). Lake area increased with local water balance and decreased with mean air temperature since snowmelt (i.e. decreased with seasonal thaw depth). Local water balance and mean air temperature since snowmelt together explained 80.7% of total variance in lake areas, and period accounted for another 14.3%. From the model output (Table III), lake area increased by 1771 ha (14.4%) in 1994 from 12 296 ha in 1984 but decreased by 1298 ha (10.6%) during 1999–2002 and showed no significant change in 2009. In Figure 3, the observed lake areas were the actual lake area obtained from Landsat images, and the predicted lake areas indicated what we should expect the lake areas to be, given the local water balance and the mean air temperature since snowmelt on those dates. The differences between the observed and predicted lake areas (residuals) indicated the lake areas that were not accounted for by the natural variability in climate, so they were considered long-term lake area change potentially caused by other factors.

### *Spatial pattern of area changes of individual lakes*

By comparing individual lake areas between period I (1984–1986) and period III (1999–2002) using the method described in section 3.4, we identified 103 expanding lakes,

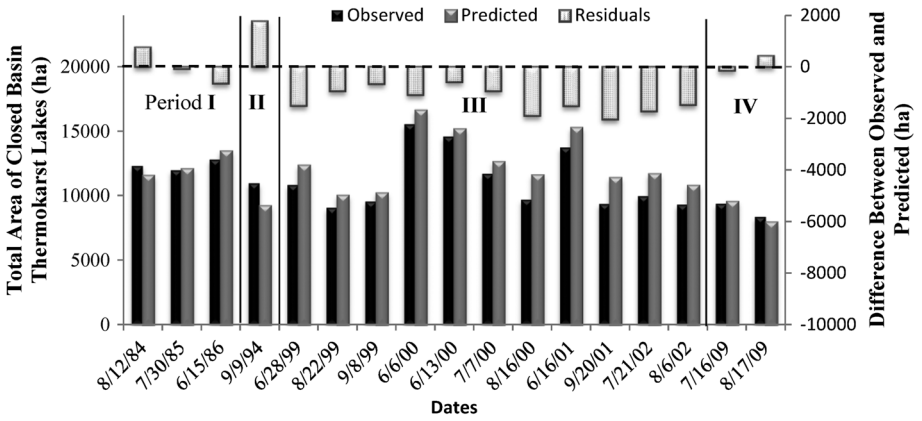


Figure 3. Total observed and predicted areas of closed basin thermokarst lakes over the study period. Predicted areas are lake areas corrected for their local water balance and mean air temperature since snowmelt (i.e. predicted area = $a + b_1$•LWB + $b_2$•MTSS, a, $b_1$, $b_2$ were obtained from Table III, LWB is the local water balance and MTSS is the mean air temperature since snowmelt). Residuals are the difference between the observed and predicted lake areas

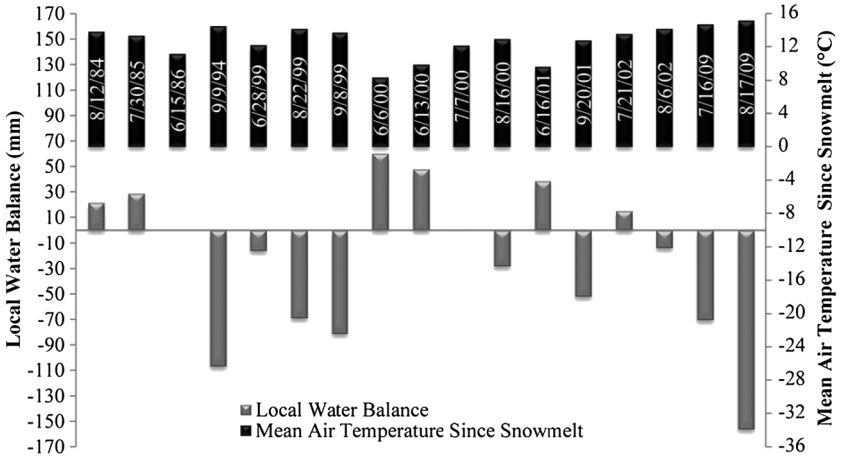


Figure 4. Local water balance and mean air temperature since snowmelt over the study period

Table III. Regression analysis of lake area and local water balance, summer mean daily temperature and periods

| Predictors[1] | | Estimates of coefficients[2] | *P* |
|---|---|---|---|
| **Intercept** | | 22658 (a) | <0.0001 |
| **Local water balance (LWB)** | | 14 ($b_1$) | 0.016 |
| **Mean daily temperature (MDT)** | | −825 ($b_2$) | <0.0001 |
| **Period (PRD)** | 1994 | 1771($b_{32}$) | 0.053 |
| | 1999-2002 | −1298 ($b_{33}$) | 0.010 |
| | 2009 | 141 ($b_{34}$) | 0.847 |

*Note*: 1. LWB, MDT and PRD are predictors and coefficients specified for regression model (Equation 2).
2. a, $b_1$, $b_2$, $b_{32}$, $b_{33}$ and $b_{34}$ are coefficients specified for regression model (Equation 2).

350 shrinking lakes and 1827 lakes without change. There was strong spatial autocorrelation in the change trends of individual lakes (Global Moran's $I = 0.01$, $p < 0.01$). Clusters of expanding lakes and shrinking lakes were identified using local spatial autocorrelation analysis (Local Moran's I), as shown in Figure 5.

The short-term variability of lakes ranged greatly among the 2280 lakes, with coefficients of variation ranging from 0.01 to 3.32. Commonly, the larger lakes were relatively stable, but the small lakes were not always variable. Along the southern boundary of the study area, lakes of all sizes exhibited low values of coefficient of variation (Figure 6). Lakes with similar variability were clustered (Figure 7). In particular, most of the stable lakes were located in the south and west of the study area, and a few stable lakes were distributed in the northeast surrounded by many variable lakes.

Figure 8 showed the long term trend from Period I (1984–1986) to Period III (1999–2002) in individual lake areas superimposed on a map of the surficial geology. There are four types of deposits mapped in the study region: floodplain, alluvial fan, alluvial terrace and upland loess. Lakes surrounded by upland loess were not included in further spatial analysis because of their small sample size ($n = 7$). Most shrinking lakes were distributed in the central part of our study area (Figure 8). In particular, large shrinking lakes were located along floodplains and alluvial terrace adjacent to floodplains, whereas small shrinking lakes were mostly located on alluvial terrace. Most expanding lakes were distributed on the floodplain of Yukon River and its tributaries. Table IV presents the results of Chi square test for independence between lake change trend and deposit types. The association between lake change trends and deposit types was statistically significant. Lakes on alluvial terrace were more likely to decrease, and lakes on floodplain were more likely to increase, as seen from their large positive adjusted standardized residuals (>2) (Agresti, 2007).

## DISCUSSION

### *Trend in lake area change*

Temporal analysis showed an increase in lake area between 1984–86 and 1994, but a decrease between 1984–86 and 1999–2002 after we accounted for the natural inter-annual and intra-annual variability caused by local water balance and mean air temperature since snowmelt. These results were consistent with the previous findings (Riordan *et al*., 2006; Corcoran *et al*., 2009; Lu and Zhuang, 2011; Rover *et al*., 2012). However, the decrease magnitude in our study was different from previous studies. Riordan *et al*. (2006) reported a lake area decrease of 21.5% for Yukon Flats National Wildlife Refuge between 1978 and 2001. Lu and Zhuang (2011) showed a lake area decrease of 4% for closed basin lakes between 1984–1989 and 1996–2001 and 12% between 1984–1989 and 2001–2003 across discontinuous permafrost region of Yukon River Basin. In our study, we observed 9.0% decrease in total lake area between Periods I and III. The main reason why different studies found different lake area changes is that we considered the intra-annual and inter-annual variability in lake areas caused by local water balance and mean air temperature since snowmelt (partial proxy for seasonal thaw depth), whereas other studies did not consider those factors, they calculated lake decrease percentage by comparing the observed lake area without taking into account the season of the images and the water balance available for the dates that the images were obtained.

Analysis of individual lake area change between Periods I and III also showed that the number of shrinking lakes

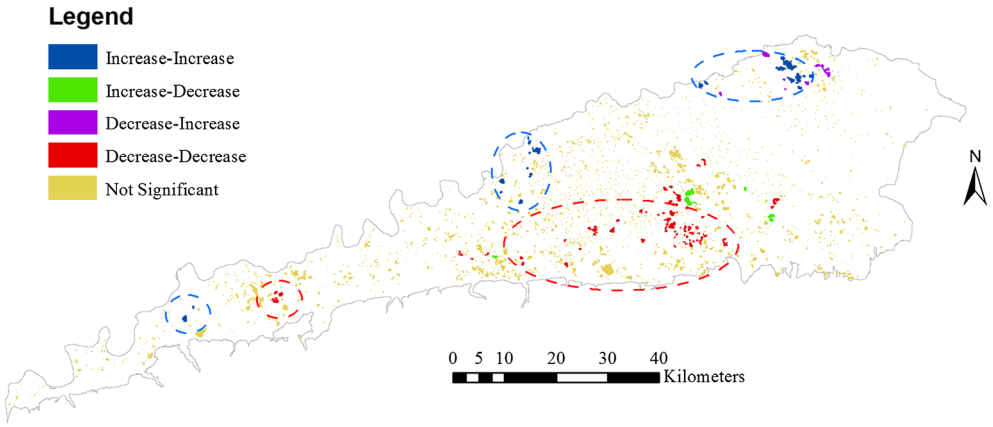


Figure 5. Lake clusters with different change trends. Lakes were color-coded in the following ways. Blue – the lake and its neighbor lakes all expanded; green – the lake expanded while its neighbor lakes shrank; purple – the lake shrank while its neighbor lakes expanded; red – the lake and its neighbor lakes all shrank; yellow – correlation of the lake and its neighbor lakes were not statistically significant

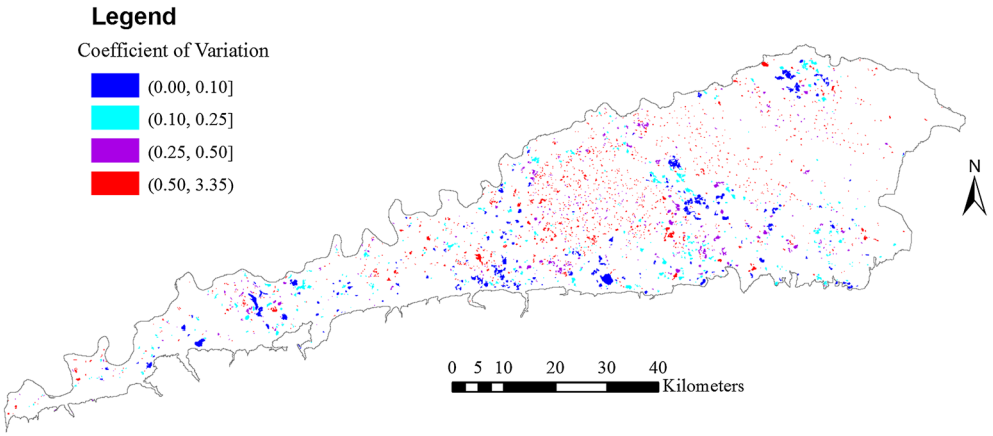


Figure 6. Coefficient of variation of individual lakes calculated from lake areas in Period III

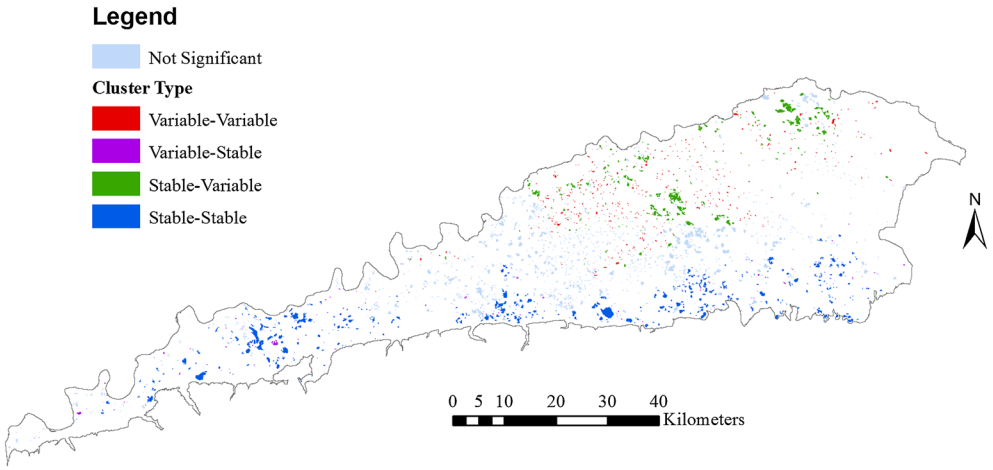


Figure 7. Lake clusters based on coefficient of variation of individual lakes for Period III. Lakes were color-coded in the following ways. Blue – the lake and its neighbor lakes were all stable; green – the lake was stable while its neighbor lakes were variable; purple – the lake was variable while its neighbor lakes were stable; red – the lake and its neighbor lakes were all variable; light blue – the correlation between the lake and its neighbor lakes was not statistically significant

(n = 350, total area decrease = 1098 ha) exceeded that of expanding lakes (n = 103, total area increase = 512 ha), resulting in a net lake area decrease of 586 ha. Spatial analysis showed that lakes with the same change trend formed clusters, with shrinking lakes mainly distributed on alluvial terrace and expanding lakes on floodplains, although some lakes with opposite change trends were adjacent to each other. This heterogeneous pattern in lake area change was also found by Riordan *et al.* (2006) and Roach *et al.* (2011). Lakes in the southern and western parts

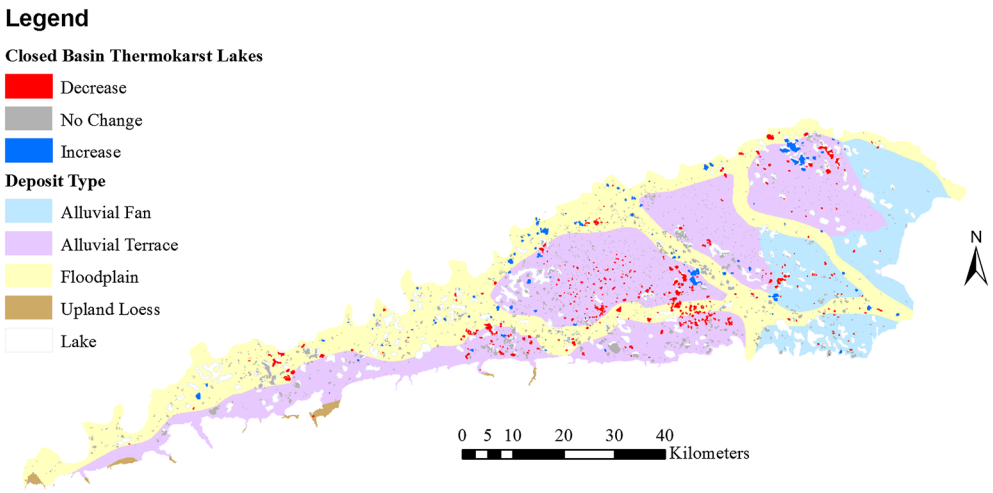


Figure 8. Change trend of closed basin thermokarst lakes and their surrounding surficial geology. Surficial geology was obtained from Surficial Geology of Alaska (U. S. Geological Survey and Karlstrom, 1964)

Table IV. Association between lake change trends and deposit types

| Observed frequency<br>Expected frequency<br>Adjusted standardized residual | | Lake change trends | | | |
|---|---|---|---|---|---|
| | | Decrease | No change | Increase | Row total |
| **Deposit types** | **Alluvial fan** | 37<br>29<br>1.6 | 151<br>152<br>−0.2 | 2<br>9<br>−2.4 | 190 |
| | **Alluvial terrace** | 226<br>197<br>3.4 | 1020<br>1027<br>−0.7 | 36<br>58<br>−4.5 | 1282 |
| | **Floodplain** | 86<br>123<br>−4.5 | 650<br>641<br>0.9 | 65<br>36<br>6.1 | 801 |
| | **Column total** | 349 | 1821 | 103 | 2273 |

Pearson's chi-squared test: chi squared = 53.9, df = 4, $p = 5.6 \times 10^{-11}$
Detailed information on Pearson's chi-squared test can be found in Agresti (2007).

of the study area seemed to be stable, whereas in the northeast part of the study area, most lakes tended to fluctuate greatly, although a few large lakes stayed stable. Similar spatial pattern in lake natural variability was also observed in the previous study (Roach, 2011).

### *Drivers for lake area change*

The area of closed basin thermokarst lakes are affected by such factors as evaporation, precipitation, flooding and permafrost distribution. Therefore, we analysed the temporal trend in those factors over the study period to find out which factors were driving the lake area change. There was no significant trend in annual mean air temperature ($p > 0.40$) from Periods I to II, II to III and I to IV, but a significant decreasing trend was observed from Periods III to IV ($p = 0.03$). In summary, there was no increase trend in air temperature that could have led to increased evaporation or region-wide permafrost degradation.

In terms of precipitation, there was no significant trend in annual precipitation either for the whole study period or between different sub-periods ($p > 0.1$, Figure 9). However, the winter snowfall (from October to April) showed a marginally significant decreasing trend ($p = 0.1111$), which may cause the amount of spring snowmelt to decrease over time.

To further explore possible long term trends in permafrost conditions, we examined ground temperature from borehole data located at the Yukon Bridge just downstream of the study area. This borehole showed no significant trend in permafrost temperature at depths of 2.3, 4.1 and 6 m ($p > 0.1$) from 1993 to 2002, indicating no permafrost degradation during that period for this location. There was a strong positive correlation between annual mean air temperature at Fairbanks and permafrost temperature at Yukon Bridge at both depths of 2.3 and 4.1 m ($p < 0.05$), which indicated that permafrost temperature at this location might be largely affected by the air temperature (rather than change in other factors such as vegetation and water body distribution). At the Yukon Bridge borehole, there was a significant increase in permafrost temperature at each depth between 1993–2002 and 2005–2009. However, the Fort Hamlin Hills fire burned this borehole area in 2004, and it was very likely

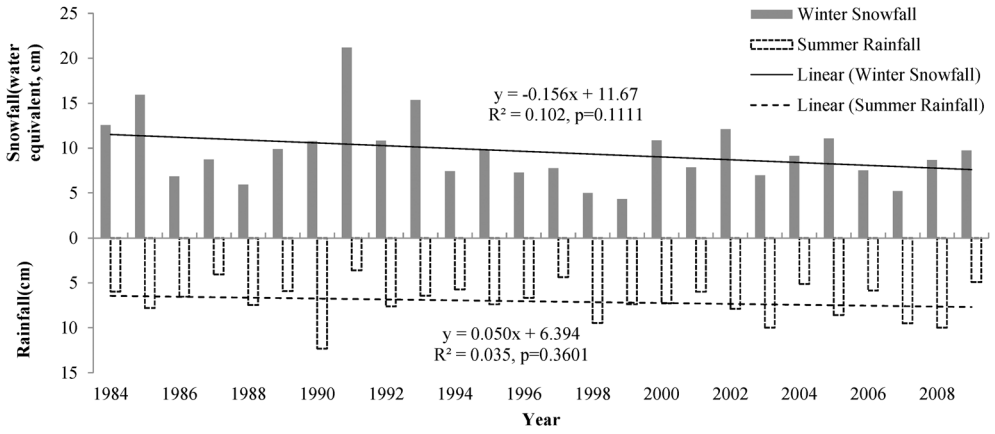


Figure 9. Annual precipitation, snowfall and rainfall at Fairbanks International Airport from 1984 to 2009

that the temperature increase after 2005 was caused by the fire and not regional trend.

Active layer depth data at three sites near Fairbanks also did not show any trend from 1990 to 2002 ($p > 0.1$). There was an increase trend at Pearl Creek ($p < 0.05$) but no significant trend at Bonanza Creek LTER or Wickersham from 2002 to 2009 ($p > 0.05$).

Although this borehole, regional air temperature and active layer data do not suggest regional permafrost degradation responsible for the lake area decrease between Period I and Period III, local changes in permafrost may have occurred because of changes in land cover such as vegetation change, occurrence of wild fires and presence of water body (Jorgenson *et al*., 2010; Rowland *et al*., 2011). Without detailed field data, it is not possible to assess local changes in permafrost conditions.

Prior studies of winter time baseflow changes (Walvoord and Striegl, 2007) and changes in the river hydrograph recession behavior (Lyon and Destouni, 2010) in the Yukon River basin have suggested that regional changes in permafrost extent and/or depth to the permafrost table have occurred in recent decades. However, there was no significant trend in recession flow intercept (a proxy for effective depth to permafrost) (Lyon and Destouni, 2010) or groundwater to stream discharge (Walvoord and Striegl, 2007) for Yukon River at Stevens Village. Therefore, there is no clear hydrologic evidence for widespread permafrost changes in our study area.

Frequency of spring ice-jam floods varied between different periods (**Table** V). The most ice-jam floods occurred between 1987 and 1994, whereas the fewest occurred between 1995 and 2002. The average frequency of ice-jam floods was marginally correlated with the average winter snowfall of each period ($R^2 = 0.80$, $p = 0.107$), suggesting that decreasing winter snowfall may be related to a decrease in ice-jam flooding frequency. Large winter snow pack that lead to high spring snowmelt flows in streams and rivers has been attributed to increases in ice-jam flooding occurrence in northern rivers (Prowse and Beltaos, 2002; Beltaos and Prowse, 2009). This ice-jam flooding frequency pattern coincided very well with the lake area change pattern, indicating that ice-jam flooding frequency change (driven by winter snowfall change) may be a significant contributor to lake area changes in the Yukon Flats. One of the concerns we had about the effects of ice-jam flooding along the Yukon River on total lake areas was that ice-jam flooding at Beaver or Fort Yukon was unlikely to cause flooding along the tributaries away from the Yukon River. However, the flooding events at Steese Highway Bridge of Birch Creek (one of the major tributaries of Yukon River that flows across our study area) from 1989 to 1994 (Kostohrys and Sterin, 1996) coincided well with the ice-jam flooding reported on the Yukon River. The spatial extent of ice-jam related flooding is not known, but it is likely that lakes located in floodplain regions would be more likely to be inundated than lakes on topographically higher alluvial terraces (Figure 8).

Ice-jam related flooding may also explain the spatial pattern of individual lake area change. In the study area, elevation is highest at the southeastern corner, and lower

Table V. Ice-jam flooding frequency and average winter snowfall

| Periods | Ice-jam flooding frequency | | | | | Average winter snowfall (cm) |
|---|---|---|---|---|---|---|
| | Number of years | Fort Yukon | Beaver village | Total | Average (per year) | |
| **1979–1986** | 8 | 3 | 0 | 3 | 0.375 | 4.1 |
| **1987–1994** | 8 | 4 | 1 | 5 | 0.625 | 4.4 |
| **1995–2002** | 8 | 0 | 0 | 0 | 0 | 3.2 |
| **2003–2009** | 7 | 2 | 0 | 2 | 0.286 | 3.3 |

toward north and west, but the east is still much higher than the west. The bigger cluster of shrinking lakes (Figure 5) was on the floodplain and adjacent alluvial terrace, close to the upper reaches of both Beaver Creek and Birch Creek, with relatively higher elevations. Lakes on higher land may receive less snowmelt water than those in lower lying areas because lower areas are more easily inundated by snowmelt. However, when flooding occurred on Beaver Creek and Birch Creek, the lakes on high land surrounding the upper reaches of the two creeks may have been recharged to a much higher water level. If they were frequently recharged by flooding, their water level should stay high and stable. Conversely, if fewer floods occurred, then they would not be recharged as often as before, resulting in a net loss in water level as well as lake area. Therefore, ice-jam flooding might be an important driver to area changes of those lakes. Similar results were found in Mackenzie River Delta, that is, shortening of river-to-lake connection times were also observed there for high closure lakes (lakes not flooded every spring because of high sill level) over a 30+ year period and was attributed to the declining effects of floods and river discharge level (Lesack and Marsh, 2007). Study of perched high closure lakes in the Mackenzie Delta (Marsh and Lesack, 1996) also showed that water level of those lakes could decline rapidly because of decrease in flood frequency.

Another possible reason for the observed pattern of lake changes might be permafrost degradation, which locally may be influenced by the lakes themselves. The presence of water body constitutes a heat source, leading to increased heat flow and temperature beneath the lake or pond so that a perennial thaw layer (talik) between the lake bottom and permafrost forms and increases in thickness over time (Burn, 2002; Ling and Zhang, 2003; Rowland *et al.*, 2011). Taliks, in turn, would cause further thaw settlement and permafrost degradation in the ground under and around thaw lakes (Johnston and Brown, 1964; Ling and Zhang, 2003). If more taliks developed in our study region beneath the lakes, then those lakes might become connected to groundwater network, leading to water exchange between lakes and groundwater. The direction that groundwater flows is determined by the slope of potentiometric surface (a hypothetical surface representing the level to which groundwater would rise if not trapped in a confined aquifer). In general, the potentiometric surface is not influenced by the surface topography and surface water features but by the structure of the confined aquifer (Fetter, 1994). In the arctic, it is permafrost that serves as the confining layer, which can be influenced by the surface topography. Lakes discharge to groundwater if the potentiometric surface is below lakes, and vice versa (Figure 10). In our results, the expanding lakes on floodplain might be recharged by groundwater and the shrinking lakes on alluvial terrace might lose water to groundwater because of their relative position to the potentiometric surface. Recent geophysical data for the Yukon Flats area indicated permafrost distribution (Minsley *et al.*, 2012) on a few transects close to the eastern boundary and center of our study area. Minsley *et al.* (2012) showed through-going talik underneath many lakes in the study area. In particular, in alluvial terrace deposits closer to the Yukon river, Canvasback Lake (see Minsley *et al.*, 2012, auxiliary material) and lakes near 12-mile lake show through-going talik underneath, and in our study we observed areal decreases in those lakes (Figure 8), consistent with drainage to the subsurface (Lake A in Figure 10).

Spatial analysis of natural variability of individual lakes in Period III (Figure 5 and Figure 6) also showed that most stable lakes were located in the southern and western parts of the study area, and the sparsely distributed stable lakes in the northeastern part were usually large and along the floodplain. In contrast, the variable lakes were mainly distributed on the alluvial terrace of the northeastern part of the study area. A regional groundwater modeling study (Walvoord *et al.*, 2012) shows consistent results with our observed spatial pattern in lake variability, that is, the Walvoord *et al.* (2012) indicates that southern part of our study area at the base of the upland loess plateau should be an area with

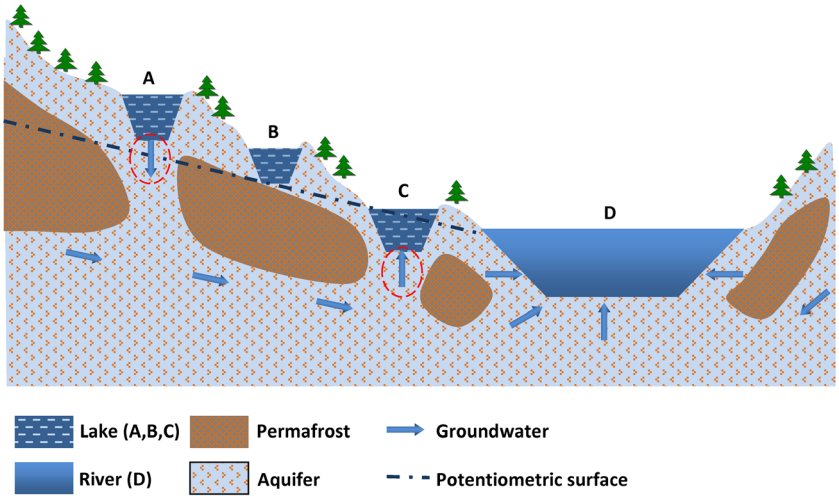


Figure 10. Sub-permafrost Groundwater flow in discontinuous permafrost region. Lake A is above potentiometric surface and recharges groundwater; Lake B is underlain by permafrost and has no connection to groundwater; Lake C is below potentiometric surface and is recharged by groundwater. River D is recharged by groundwater

upward head gradients, suggesting groundwater recharge into lakes through sub-lake taliks, which helps to explain why we observe lakes with stable areas and no long-term trends (Figure 7and Figure 8) in this same region.

We also found that among 103 expanding lakes, 78 lakes (76%) had low natural variability (CV $< 0.20$, a criterion used by previous studies (Roach, 2011)), whereas among 350 shrinking lakes, 274 lakes (78%) had high natural variability (CV $> 0.20$). These associations between lake variability and change trends may have implications of local permafrost degradation. Specifically, when talik thawed through permafrost beneath lakes because of the heating effects of lakes themselves and became connected to groundwater system, lakes at lower elevations or with upwelling gradient were likely to be recharged by groundwater and stayed stable. In contrast, lakes at higher elevations or with downward hydraulic gradient were likely to lose water to groundwater and fluctuated greatly between different seasons and years.

In addition, Roach (2011) pointed out that when permafrost thawed, lakes in coarse-grain sandy soils may be more likely to shrink, whereas fine-grained fluvial soils may be more susceptible to subsidence events because of their higher ice content and thus may promote lake expansion. In our study area, the soils were described as poorly drained and commonly overlain by peat on flats areas away from the main river channels, although the soils were better drained on natural levees, consisting of silty and sandy sediments (Brabets *et al*., 2000) at a regional level. However, no fine-scale map or description of soil types is available, which makes it difficult to determine whether shrinking of certain lakes was because of coarse-grain sandy soils, and expansion of other lakes was caused by disappearance of ice content in fine-grained fluvial soils.

From the temporal and spatial patterns of lake area changes in our study area, we hypothesized ice-jam flooding and local permafrost degradation may be two important contributors to those patterns. Permafrost distributions beneath the lakes and hydraulic head gradient of lakes relative to groundwater table may be the dominant driver for the spatial pattern of lake variability. However, more field-based site knowledge is required, such as observation of how ice-jam flooding influences those lakes in spring and effective horizontal and vertical mapping of permafrost beneath and around the lakes.

## CONCLUSION

In this study, we used Landsat images of 17 dates from 1984 to 2009 to detect long-term change in closed basin thermokarst lake areas for a study area within Yukon Flats, Alaska, by using a multiple linear regression model with consideration of the natural intra-annual and inter-annual variability in lake area. We found that 80.7% of variation in lake areas of 17 dates was explained by local water balance and mean air temperature since snowmelt (interpreted as a proxy for seasonal thaw depth) and another 14.3% of variation was accounted for by different periods. When we accounted for the effect of local water balance and mean air temperature since snowmelt on intra-annual and inter-annual variability in lake areas in the multiple regression analysis, we found that lake area increased by 14.4% in 1994 but decreased by 10.6% during 1999–2002, compared with the 1984 area of 12 296 ha. Among the 2280 closed basin thermokarst lakes, 350 lakes showed an area decrease, and 103 lakes showed an increase between 1984–1986 (Period I) and 1999–2002 (Period III). The expanding lakes were mainly distributed along the floodplain of Yukon River and its tributaries, whereas the shrinking lakes were located on alluvial terraces. By analysing potential factors driving lake area change including evaporation, precipitation, regional permafrost degradation, and ice-jam flooding, we found that there was no evidence of region-wide permafrost degradation. Instead, fluctuating ice-jam flooding frequency might be an important driver for the observed temporal spatial lake area change pattern. Local permafrost distribution might be the driver for the spatial pattern of lake variability and local permafrost degradation might be another factor affecting the spatial pattern of lake area change.

## ACKNOWLEDGEMENT

Funding for this research was provided by the Department of Energy Office of Science, Office of Biological and Environmental Research. Borehole data on permafrost temperature was provided by NCAR/EOL under sponsorship of the National Science Foundation. We are thankful for the helpful comments and suggestions provided by two anonymous reviewers and Editor Malcolm G Anderson. We also thank Lauren M. Charsley-Groffman for her help with extraction of lakes from Landsat images.

## REFERENCES

Adlam LS, Balks MR, Seybold CA, Campbell DI. 2010. Temporal and spatial variation in active layer depth in McMurdo Sound Region, Antarctica. *Antarctic Science* **22**: 45–52. doi: 10.1016/S0921-8181(03)00106-1.

Agresti A. 2007. *An Introduction to Categorical Data Analysis*, John Wiley & Sons, Inc.: Hoboken, NJ, USA.

Anderson L, Abbott MB, Finney BP, Burns SJ. 2007. Late Holocene moisture balance variability in the Southwest Yukon Territory, Canada. *Quaternary Science Reviews* **26**: 130–141. doi: 10.1111/j.1538-4632.1995.tb00338.x.

Anselin L. 1995. Local indicators of spatial association: LISA. *Geographical Analysis* **27**: 93–115. doi: 10.1111/j.1538-4632.1995.tb00338.x.

Arp CD, Jones BM. 2009. Geography of Alaska lake districts: Identification, description, and analysis of lake-rich regions of a diverse and dynamic state. U.S. Geological Survey Scientific Investigations Report. 2008–5215; 40 p.

Arp CD, Jones BM, Urban FE, Grosse G. 2011. Hydrogeomorphic processes of thermokarst lakes with grounded-ice and floating-ice regimes on the Arctic Coastal Plain, Alaska. *Hydrological Processes* **25**: 2422–2438. doi: 10.1002/hyp.8019.

Beltaos S, Prowse T. 2009. River-ice hydrology in a shrinking cryosphere. *Hydrological Processes* **23**: 122–144. doi: 10.1002/hyp.7165.

Bockheim JG, Campbell IB, McLeod M. 2007. Permafrost distribution and active-layer depths in the McMurdo Dry Valleys,Antarctica. *Permafrost and Periglacial Processes* **18**: 217–227. doi: 10.1002/ppp.588.

Bowling LC, Lettenmaier DP. 2010. Modeling the effects of lakes and wetlands on the water balance of arctic environment. *Journal of Hydrometeorology* **11**: 276–295. doi: 10.1175/2009JHM1084.1.

Bowling LC, Kane DL, Gieck RE, Hinzman LD, Lettenmaier DP. 2003. The role of surface storage in a low-gradient Arctic watershed. *Water Resource Research* **39**: 1087. doi: 10.1029/2002wr001466.

Boyd WL. 1959. Limnology of selected arctic lakes in relation to water supply problems. *Ecology* **40**: 49–54. doi: 10.2307/1929921.

Brabets TP, Wang B, Meade RH. 2000. Environmental and Hydrologic Overview of the Yukon River Basin, Alaska and Canada. Water-Resources Investigations Report. U.S. Department of the Interior. U.S. Geological Survey. 99–44204; 106 p.

Brumby SP, Theiler J, Perkins SJ, Harvey NR, Szymanski JJ, Bloch JJ, Mitchell M. 1999. Investigation of image feature extraction by a genetic algorithm. *Proceedings of SPIE* **3812**: 24–31. doi: 10.1117/12.367697.

Brutsaert W, Yeh G-T. 1970. Implications of a type of empirical evaporation formula for lakes and pans. *Water Resources Research* **6**: 1202–1208. doi: 10.1029/WR006i004p01202.

Burn CR. 2002. Tundra lakes and permafrost, Richards Island, Western Arctic Coast, Canada. *Canadian Journal of Earth Sciences* **39**: 1281–1298. doi: 10.1139/e02-035.

Chen M, Rowland JC, Wilson CJ, Altmann GL, Brumby SP. In Review. Understanding intra-annual and inter-annual lake area change dynamics in Yukon Flats, Alaska. *Permafrost and Periglacial Processes*.

Conovitz PA, MacDonald LH, McKnight DM. 2006. Spatial and temporal active layer dynamics along three glacial meltwater streams in the McMurdo Dry Valleys, Antarctica. *Arctic, Antarctic, and Alpine Research* **38**: 42–53.

Corcoran RM, Lovvorn JR, Heglund PJ. 2009. Long-term change in limnology and invertebrates in Alaskan boreal wetlands. *Hydrobiologia* **620**: 77–89. doi: 10.1007/s10750-008-9616-5.

Cott PA, Sibley PK, Gordon AM, Bodaly RA, Mills KH, Somers WM, Fillatre GA. 2008. Effects of water withdrawal from ice-covered lakes on oxygen, temperature, and fish. *Journal of the American Water Resources Association* **44**: 328–342. doi: 10.1111/j.1752-1688.2007.00165.x.

Davydov SP, Fyodorov-Davydov DG, Neff JC, Shiklomanov NI, Davydova AI. 2008. Changes in active layer thickness and seasonal fluxes of dissolved organic carbon as a possible baseline for permafrost monitoring. *In Proceedings of the Ninth International Conference on Permafrost*, Kane DL, Hinkel KM (eds.), Institute of Northern Engineering, University of Alaska: Fairbanks, AK, USA; 333–336.

Fetter CW. 1994. *Applied Hydrogeology*, Prentice-Hall, Inc.: Upper Saddle River, NJ, USA.

Finch JW, Gash JHC. 2002. Application of a simple finite difference model for estimating evaporation from open water. *Journal of Hydrology* **255**: 253–259. doi: 10.1016/j.bbr.2011.03.031.

Ford J, Bedford BL. 1987. The Hydrology of Alaskan Wetlands, U.S.A.: A Review. *Arctic and Alpine Research* **19**: 209–229.

Frohn RC, Hinkel KM, Eisner WR. 2005. Satellite remote sensing classification of thaw lakes and drained thaw lake basins on the North Slope of Alaska. *Remote Sensing of Environment* **97**: 116–126. doi: 10.1016/j.rse.2005.04.022.

Guglielmin M. 2004. Observations on permafrost ground thermal regimes from Antarctica and the Italian Alps, and their relevance to global climate change. *Global and Planetary Change* **40**: 159–167. doi: 10.1016/S0921-8181(03)00106-1.

Harvey NR, Theiler J, Brumby SP, Perkins S, Szymanski JJ, Bloch JJ, Porter RB, Galassi M, Young AC. 2002. Comparison of GENIE and conventional supervised classifiers for multispectral image feature extraction. *Geoscience and Remote Sensing, IEEE Transactions on Geoscience and Remote Sensing* **40**: 393–404. doi: 10.1109/36.992801.

Hinkel KM, Paetzold F, Nelson FE, Bockheim JG. 2001. Patterns of soild temperature and moisture in the active layer and upper permafrost at Barrow, Alaska: 1993–1999. *Global and Planetary Change* **29**: 293–309. doi: 10.1016/S0921-8181(01)00096-0.

Hinkel KM, Frohn RC, Nelson FE, Eisner WR, Beck RA. 2005. Morphometric and spatial analysis of thaw lakes and draind thaw lake basins in the Western Arctic Coastal Plain, Alaska. *Permafrost and Periglacial Processes* **16**: 327–341. doi: 10.1002/ppp.532.

Hinzman LD, Bettez ND, Bolton WR, Chapin FS, Dyurgerov MB, Fastie CL, Griffith B, Hollister RD, Hope A, Huntington HP, Jensen AM, Jia GJ, Jorgenson T, Kane DL, Klein DR, Kofinas G, Lynch AH, Lloyd AH, McGuire AD, Nelson FE, Oechel WC, Osterkamp TE, Racine CH, Romanovsky VE, Stone RS, Stow DA, Sturm M, Tweedie CE, Vourlitis GL, Walker MD, Walker DA, Webber PJ, Welker JM, Winker KS, Yoshikawa K. 2005. Evidence and implications of recent climate change in northern Alaska and other arctic regions. *Climatic Change* **72**: 251–298. doi: 10.1007/s10584-005-5352-2.

Johnston GH, Brown RJE. 1964. Some observations on permafrost distribution at a lake in the Mackenzie delta. *Arctic* **17**: 162–175.

Jones B, Arp C, Hinkel K, Beck R, Schmutz J, Winston B. 2009. Arctic lake physical processes and regimes with implications for winter water availability and management in the National Petroleum Reserve Alaska. *Environmental Management* **43**: 1071–1084. doi: 10.1007/s00267-008-9241-0.

Jones BM, Grosse G, Arp CD, Jones MC, Anthony KW, Romanovsky VE. 2011. Modern thermokarst lake dynamics in the continuous permafrost zone, Northern Seward Peninsula, Alaska. *Journal of Geophysical Research* **116**: G00M03. doi: 10.1029/2011JG001666.

Jorgenson MT, Osterkamp TE. 2005. Response of boreal ecosystems to varying modes. *Canadian Journal of Forest Research* **35**: 2100–2111. doi: 10.1139/x05-153.

Jorgenson TM, Racine CH, Walters JC, Osterkamp TE. 2001. Permafrost degradation and ecological changes associated with a warming climate in central Alaska. *Climatic Change* **48**: 551–579.

Jorgenson TM, Yoshikawa K, Kanevskiy M, Shur YL, Romanovsky V, Marchenko S, Grosse G, Brown J, Jones B. 2008. Permafrost characteristics of Alaska. In *Proceedings of the Ninth International Conference on Permafrost*, Kane DL, Hinkel KM (eds.), Fairbanks, AK; 121–122.

Jorgenson MT, Romanovsky V, Harden J, Shur Y, O'Donnell J, Schuur EAG, Kanevskiy M, Marchenko S. 2010. Resilience and vulnerability of permafrost to climate change. *Canadian Journal of Forest Research* **40**: 1219–1236. doi: 10.1139/X10-060.

Kling G, Kipphut G, Miller M. 1992. The flux of $CO_2$ and $CH_4$ from lakes and rivers in arctic Alaska. *Hydrobiologia* **240**: 23–36. doi: 10.1007/bf00013449.

Kostohrys J, Sterin BBG. 1996. Water resources of Birch Creek National Wild river, Alaska: stream gaging data from 1989 to 1994. U.S. Bureau of Land Management, Alaska State Office. 30 p.

Labrecque S, Lacelle D, Duguay CR, Lauriol B, Hawkings J. 2009. Contemporary (1951–2001) evolution of lakes in the Old Crow Basin, Northern Yukon, Canada: Remote Sensing, numerical modeling, and stable isotope analysis. *Arctic* **62**: 225–238.

Lesack LFW, Marsh P. 2007. Lengthening plus shortening of river-to-lake connection times in the Mackenzie River Delta Respectively via two global change mechanisms along the Arctic Coast. *Geophysical Research Letters* **34**: L23404. doi: 10.1029/2007GL031656.

Lewkowicz AG, Etzelmüller B, Smith SL. 2011. Characteristics of discontinuous permafrost based on ground temperature measurements and electrical resistivity tomography, Southern Yukon, Canada. *Permafrost and Periglacial Processes* **22**: 320–342. doi: 10.1002/ppp.703.

Ling F, Zhang T. 2003. Numerical simulation of permafrost thermal regime and talik development under shallow thaw lakes on the Alaskan Arctic Coastal Plain. *Journal of Geophysical Research* **108**: 4511. doi: 10.1029/2002JD003014.

Lu X, Zhuang Q. 2011. Areal changes of land ecosystems in the Alaskan Yukon River Basin from 1984 to 2008. *Environmental Research Letters* **6**: 034012. doi: 10.1088/1748-9326/6/3/034012.

Lyon SW, Destouni G. 2010. Changes in catchment-scale recession flow properties in response to permafrost thawing in the Yukon River Basin. *International Journal of Climatology* **30**: 2138–2145. doi: 10.1002/joc.1993.

Mackay RJ. 1995. Active layer changes (1968 to 1993) following the forest-tundra fire near Inuvik, N.W.T., Canada. *Arctic and Alpine Research* **27**: 323–336.

Marsh P, Lesack LFW. 1996. The hydrologic regime of perched lakes in the Mackenzie delta: Potential responses to climate change. *Limnology and Oceanography* **41**: 849–856.

McGarigal K, Cushman SA, Neeland MC, Ene E. 2002. *FRAGSTATS: Spatial Pattern Analysis Program for Categorical Maps*. University of Massachusetts: Amherst, MA, USA.

Menard S. 1995. *Applied Logistic Regression Analysis: Sage University Series on Quantitative Applications in the Social Sciences*, Sage Publications, Inc.: Thousand Oak, CA, USA.

Minsley BJ, Abraham JD, Smith BD, Cannia JC, Voss CI, Johansson MT, Walvoord MA, Wylie BK, Anderson L, Ball LB, Deszcz-Pan M, Wellman TP, Ager TA. 2012. Airborne electromagnetic imaging of discontinuous permafrost. *Geophysical Research Letters* **39**: L02503. doi: 10.1029/2011GL050079

Neter J, Kutner MH, Machtsheim CJ, Wasserman W. 1996. *Applied Linear Regression Models*, McGraw-Hill Companies, Inc.: Chicago, IL, USA.

Osterkamp TE. 2007. Characteristics of the recent warming of permafrost in Alaska. *Journal of Geophysical Research* **112**: F02S02. doi: 10.1029/2006JF000578.

Osterkamp TE, Romanovsky VE. 1999. Evidence for warming and thawing of discontinuous permafrost in Alaska. *Permafrost and Periglacial Processes* **10**: 17–37.

Payne RE. 1972. Albedo of the sea surface. *Journal of The Atmospheric Sciences* **29**: 959–970.

Perkins SJ, Edlund K, Esch-Mosher D, Eads D, Harvey N, Brumby S. 2005. Genie Pro: Robust image classification using shape, texture, and spectral information. *Proceedings of SPIE* **5806**: 139–148. doi: 10.1117/12.604519.

 

Plug LJ, Walls C, Scott BM. 2008. Tundra lake changes from 1978 to 2001 on the Tuktoyaktuk Peninsula, western Canadian Arctic. *Geophysical Research Letters* **35**: L03502. doi: 10.1029/2007gl032303.

Prowse TD, Beltaos S. 2002. Climatic control of river-ice hydrology: a review. *Hydrological Processes* **16**: 805–822. doi: 10.1002/hyp.369.

Riordan B, Verbyla D, McGuire AD. 2006. Shrinking ponds in subarctic Alaska based on 1950–2002 remotely sensed images. *Journal of Geophysical Research* **111**: G04002. doi: 10.1029/2005JG000150.

Roach J. 2011. Lake Area Change in Alaskan National Wildlife Refuges: Magnitude, Mechanisms, and Heterogeneity. PhD Thesis. University of Alaska: Fairbanks, AK, USA; 225 p.

Roach J, Griffith B, Verbyla D, Jones J. 2011. Mechanisms influencing changes in lake area in Alaskan boreal forest. *Global Change Biology* **17**: 2567–2583. doi: 10.1111/j.1365-2486.2011.02446.x.

Rovansek RJ, Hinzman LD, Kane DL. 1996. Hydrology of a tundra wetland complex on the Alaskan Arctic Coastal Plain, U.S.A. *Arctic and Alpine Research* **28**: 311–317. doi: 10.2307/1552110.

Rover J, Ji L, Wylie BK, Tieszen LL. 2012. Establishing water body areal extent trends in interior Alaska from multi-temporal Landsat data. *Remote Sensing Letters* **3**: 595–604. doi: 10.1080/01431161.2011.643507.

Rowland JC, Travis BJ, Wilson CJ. 2011. The role of advective heat transport in talik development beneath lakes and ponds in discontinuous permafrost. *Geophysical Research Letters* **38**: L17504. doi: 10.1029/2011GL048497.

Shuttleworth WJ. 2012. *Terrestrial Hydrometeorology*, John Wiley & Sons, Ltd: Hoboken, NJ, USA.

Smith LC, Sheng Y, MacDonald GM. 2007. A first pan-Arctic assessment of the influence of glaciation, permafrost, topography and peatlands on northern hemisphere lake distribution. *Permafrost and Periglacial Processes* **18**: 201–208. doi: 10.1002/ppp.581.

U. S. Geological Survey, Karlstrom TNV. 1964. Surficial Geology of Alaska. Department of the Interior, U.S. Geological Survey. Washington, D.C., USA.

Walvoord MA, Striegl RG. 2007. Increased groundwater to stream discharge from permafrost thawing in the Yukon River Basin: Potential impacts on lateral export of carbon and nitrogen. *Geophysical Research Letters* **34**: L12402. doi: 10.1029/2007GL030216.

Walvoord MA, Voss CI, Wellman TP. 2012. Influence of permafrost distribution on groundwater flow in the context of climate-change-driven permafrost thaw: Example from Yukon Flats Basin, Alaska, USA. *Water Resource Research* doi: 10.1029/2011WR011595.

Williams JR. 1962. Geologic Reconaissance of the Yukon Flats District, Alaska. *U.S. Geological Survey Bulletin* **1 1 1 1-H**.

Woo M-K, Guan XJ. 2006. Hydrological connectivity and seasonal storage change of tundra ponds in a polar oasis environment, Canadian High Arctic. *Permafrost and Periglacial Processes* **17**: 309–323. doi: 10.1002/ppp.565.

Yoshikawa K, Hinzman LD. 2003. Shrinking thermokarst ponds and groundwater dynamics in discontinuous permafrost near Council, Alaska. *Permafrost and Periglacial Processes* **14**: 151–160. doi: 10.1002/ppp.451.

Zhang T, Osterkamp TE, Stamnes K. 1997. Effects of climate on the active layer and permafrost on the North Slope of Alaska, U.S.A. *Permafrost and Periglacial Processes* **8**: 45–67.

 